

Endergonic synthesis driven by chemical fuelling

Received: 31 October 2023

Accepted: 1 February 2024

Published online: 11 March 2024

 Check for updatesEnzo Olivieri ^{1,3}, James M. Gallagher ^{1,3}, Alexander Betts ¹,
Toufic W. Mrad ¹ & David A. Leigh ^{1,2} 

Spontaneous chemical reactions proceed energetically downhill to either a local or global minimum, limiting possible transformations to those that are exergonic. Endergonic reactions do not proceed spontaneously and require an input of energy. Light has been used to drive a number of deracemizations and thermodynamically unfavourable bond-forming reactions, but is restricted to substrates that can absorb, directly or indirectly, energy provided by photons. In contrast, anabolism involves energetically uphill transformations powered by chemical fuels. Here we report on the transduction of energy from an artificial chemical fuel to drive a thermodynamically unfavourable Diels–Alder reaction. Carboxylic acid catalysed carbodiimide-to-urea formation is chemically orthogonal to the reaction of the diene and dienophile, but transiently brings the functional groups into close proximity, causing the otherwise prohibited cycloaddition to proceed in modest yield (15% after two fuelling cycles) and with high levels of regio- (>99%) and stereoselectivity (92:8 *exo:endo*). Kinetic asymmetry in the fuelling cycle ratchets the Diels–Alder reaction away from the equilibrium distribution of the Diels–Alder:retro-Diels–Alder products. The driving of the endergonic reaction occurs through a ratchet mechanism (an energy or information ratchet, depending on the synthetic protocol), reminiscent of how molecular machines directionally bias motion. Ratcheting synthesis has the potential to expand the synthetic chemistry toolbox in terms of reactivity, complexity and control.

Biological anabolism is the construction of large, often functional-group-rich, molecules from simpler available building blocks. These structurally complex products typically have a higher chemical potential than the starting materials¹, meaning that ‘contra-thermodynamic’ transformations need to be coupled to exergonic processes to satisfy the conservation of energy^{3–5}. Many synthetic schemes in biology involve the energy-demanding reaction being chemically orthogonal to the energy-releasing reaction that drives it^{5–9}. This ubiquitous ‘chemical fuelling’ strategy allows both the synthesis of adenosine triphosphate (ATP) from chemically unrelated redox reactions^{6,7}, and the subsequent use of ATP as a universal energy currency to drive

numerous transformations⁹ in biological metabolism. Energy transduction between two unrelated chemical reactions becomes possible when the endergonic process is a catalyst^{3,10} for the exergonic process. In this way a ratchet mechanism^{11–20} provides the means of transducing an energy input into the chemical work necessary for endergonic synthesis^{3,4,10,20}. In molecular-level machinery, ratchet mechanisms rectify stochastic fluctuations to accomplish directional motion^{10–14}. In this Article, we demonstrate that an autonomous chemical reaction that proceeds through thermal activation back-and-forth across transition states^{21–23} can also be rectified by a ratchet mechanism to enable a thermodynamically unfavourable reaction outcome (Fig. 1b)³.

¹Department of Chemistry, University of Manchester, Manchester, UK. ²School of Chemistry and Molecular Engineering, East China Normal University, Shanghai, China. ³These authors contributed equally: Enzo Olivieri, James M. Gallagher. ✉ e-mail: david.leigh@manchester.ac.uk

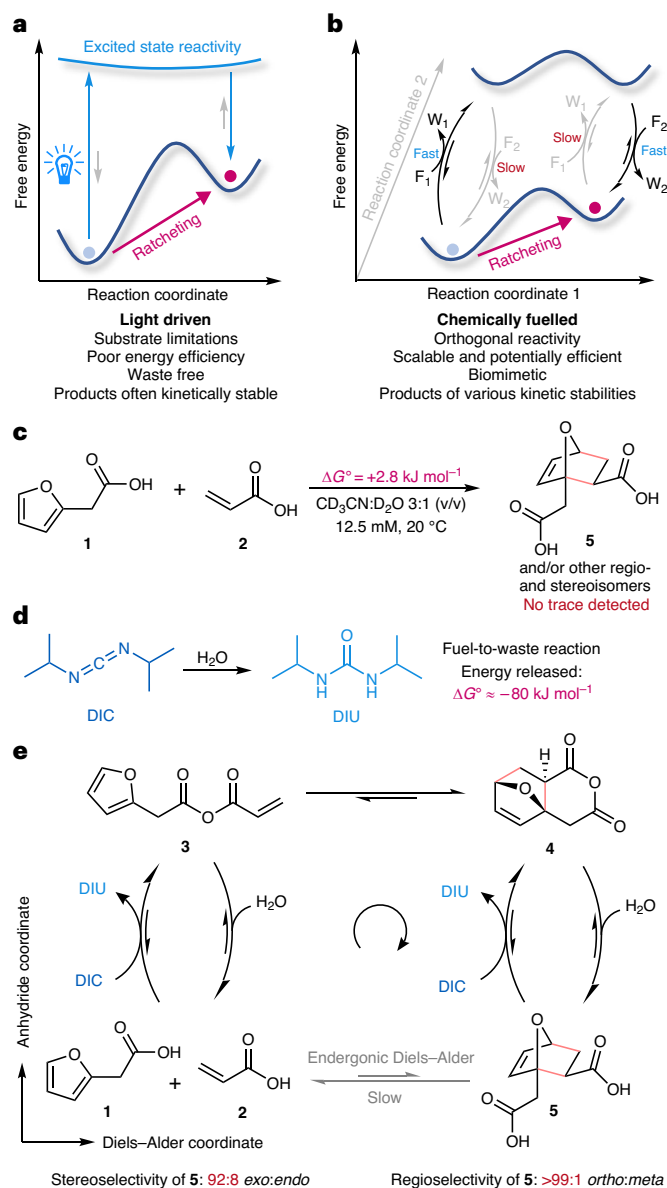


Fig. 1 | Endergonic synthesis using ratchet mechanisms. **a**, Typical endergonic chemical transformation, for example, a deracemization or isomerization reaction, driven by light. Differences in the rates of photon absorption and excited-state relaxation lead to kinetic asymmetry in the reaction cycle, driving the system away from equilibrium. **b**, Chemical fuelling of an energetically uphill chemical transformation. An endergonic process in reaction coordinate 1 can be driven by orthogonal chemical fuelling along reaction coordinate 2. In a continuous process, energy transduction is driven by an information ratchet mechanism that relies on kinetic asymmetry in the rates of the fuel-to-waste reactions ($F_1 \rightarrow W_1$ and $F_2 \rightarrow W_2$). **c**, An endergonic Diels–Alder reaction between 2-furanacetic acid and acrylic acid. No Diels–Alder adducts (neither **5** nor other possible regio- and stereoisomers) were detected by ^1H NMR or mass spectrometry from an initial concentration of 12.5 mM **1/2**. The equilibrium constant, K , determined for $1 + 2 \rightleftharpoons 5$ was 0.31 M^{-1} (Supplementary Information Section 2), meaning that at 12.5 mM the ratio (**1 + 2**):**5** is ~250:1. **d**, Free energy of fuel-to-waste reaction; the hydration of DIC ($\text{DIC} + \text{H}_2\text{O} \rightarrow \text{DIU}$)⁶². **e**, Driving the endergonic Diels–Alder reaction of **1** and **2** thermodynamically uphill under autonomous chemical fuelling.

Light energy has been used to power a number of endergonic chemical transformations^{2,24}, including deracemizations^{25–27} and double-bond isomerizations^{28–30} (Fig. 1a). However, light-driven endergonic reactions are restricted to substrates that can interact with light, generally through energy transfer or photoredox interactions^{2,24}, and

the transduction of energy to the driven reaction is generally inefficient (a typical blue-light deracemization requires only $+1.7 \text{ kJ mol}^{-1}$ of energy² yet consumes -270 kJ mol^{-1} per photon). Even the most exquisite example of light-driven endergonic synthesis, photosynthesis, has an energy efficiency of just 3–6% (ref. 31).

Chemical fuelling^{15–20,32} (Fig. 1b) mediates many synthetic processes in biology^{5–9,33,34}, can be energy efficient²⁰ and scalable, and is amenable to many different classes of substrates. However, aside from a small number of deracemization reactions^{35–37}, and a stepwise synthesis of a hydrazone using ATP³⁸, artificial autonomous chemically fuelled endergonic synthesis has remained elusive. We sought to explore whether an endergonic example of a classical chemical transformation, the Diels–Alder reaction³⁹, could be driven by chemical fuelling. The transduction of chemical energy from carbodiimide hydration through catalysis has recently been used to deracemize atropisomeric 1-(6'-substituted-phenyl)pyrrole 2,2'-dicarboxylic acid derivatives (and directionally drive rotation of the corresponding 6'-unsubstituted molecular motor)³⁵. Transient tethering of the two carboxylic acids of the biaryl catalyst to form an anhydride enables atropisomer interconversion, with kinetic asymmetry^{10,13–20} in the fuelling cycle (generated by the use of a chiral carbodiimide and chiral hydrolysis promoter) driving the endergonic deracemization³⁵. We hypothesized that similar transient tethering could be used to bring a diene and dienophile into close proximity⁴⁰, promoting an otherwise endergonic Diels–Alder reaction by organizing the reactants for the cycloaddition and substantially increasing the effective concentration. In an energy ratchet mechanism (which cyclically switches the relative heights and depths of energy minima and maxima¹¹) this could produce a power stroke that thermodynamically favoured the Diels–Alder reaction in the tethered state; in an information ratchet mechanism¹¹, any kinetic asymmetry in the rates that the starting materials and product react with the fuel (and/or waste) would drive the Diels–Alder:retro-Diels–Alder ratio away from the equilibrium value^{3,10,20}. Transiently organizing the reactants through fuelling also has the potential to exert regio- and/or stereocontrol in the driven reaction⁴¹.

Results and discussion

The Diels–Alder reaction is a synthetically important transformation in which six-membered rings are formed with up to four new stereocentres³⁹. The cycloaddition can be accelerated and the stereochemical outcome controlled by catalysts⁴²; however the yield and regio- and stereoselectivity of the reaction can all be limited by unfavourable thermodynamics^{41,43}. Temporary tethering groups have been used to improve the regio- and stereochemical outcome of Diels–Alder reactions, but adding and removing the tether requires an additional two or three synthetic steps^{41,44,45}. The intermolecular Diels–Alder reaction of furans and acrylates often favours the diene and dienophile, leading to low levels of the Diels–Alder adduct at equilibrium^{46,47}. Furthermore, the symmetry of the furan offers little electronic polarization, leading to poor regioselectivity in reactions that do proceed^{46,47}. Carrying out the reaction at elevated temperatures is also problematic due to the propensity of furans to thermally decompose. As such, this class of substrates provides a good testing ground to explore the effects and efficacy of chemical fuelling on a challenging endergonic reaction.

We chose 2-furanacetic acid (**1**) and acrylic acid (**2**) as diene and dienophile respectively (Fig. 1c). Each building block contains a carboxylic acid for forming an intermolecular anhydride, and molecular modelling suggested that the length between the diene and dienophile when tethered would not be strained when adopting the tricyclic transition state required for the cycloaddition. (Indeed, in preliminary experiments chemical fuelling of analogous acid pairs with one fewer or one more carbon atom in the chains did not lead to the formation of Diels–Alder adducts.) The transient formation of anhydrides and esters by carbodiimides in the presence of water has been exploited in

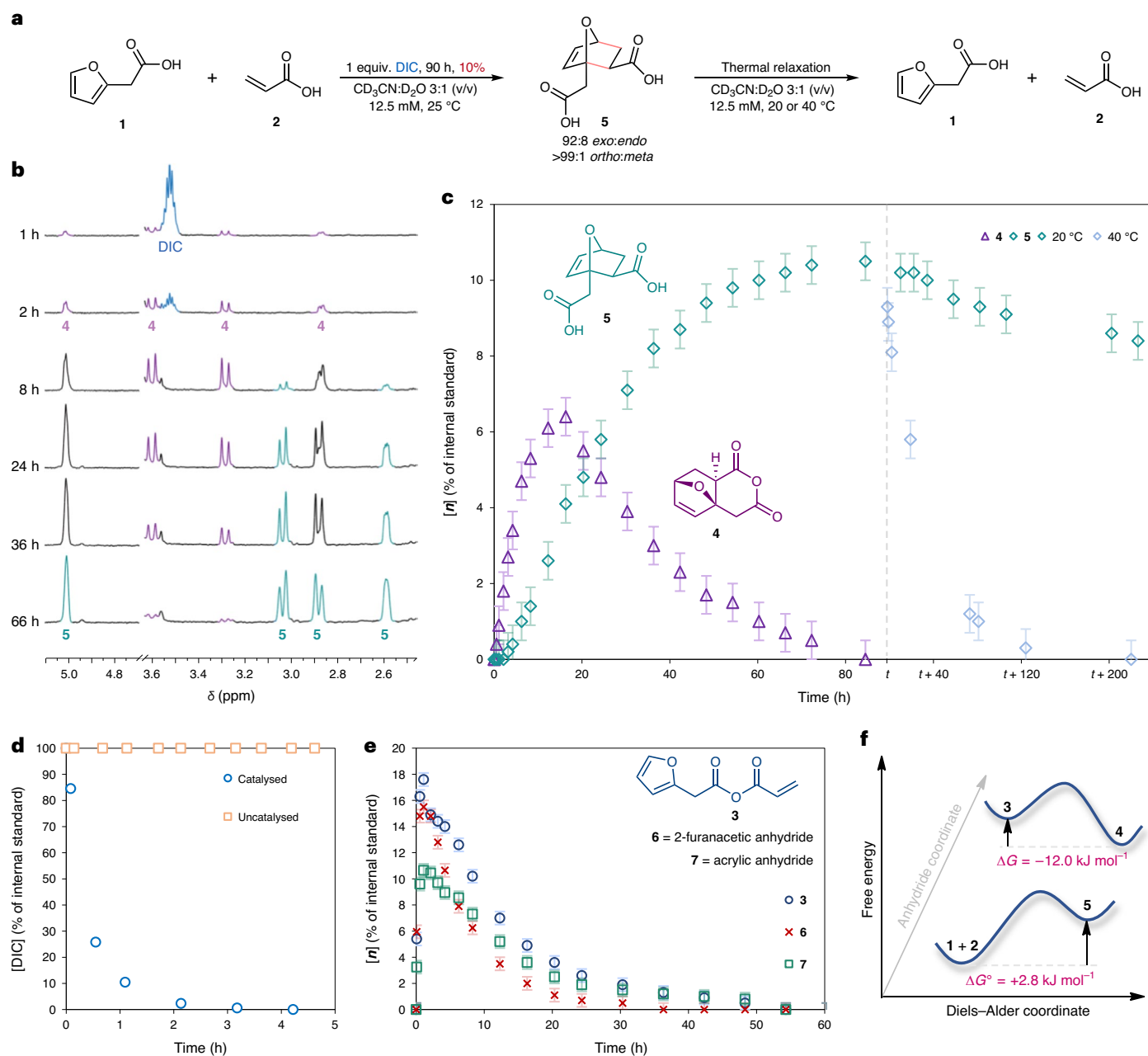


Fig. 2 | Ratcheted synthesis of 5. **a**, Ratcheted synthesis of 5 and, in the absence of the chemical fuel, its relaxation to the equilibrium distribution under the same conditions. **b**, Partial ^1H NMR (600 MHz, $\text{CD}_3\text{CN}:\text{D}_2\text{O}$ 3:1 (v/v), 298 K) stackplot showing the consumption of DIC (blue) and the formation of 4 (purple) and 5 (teal) over time. DIC addition at $t = 0$. **c**, Kinetics of the formation of 4 (triangles) and 5 (diamonds) and the subsequent retro-Diels–Alder of 5 to 1 and 2 at 20 °C or 40 °C beginning at time t . Thermal relaxation $t_{1/2}^{20^\circ\text{C}} = 16$ days, $t_{1/2}^{40^\circ\text{C}} = 25$ h. **d**, Kinetics of carbodiimide hydration catalysed by the endergonic reaction $1 + 2 \rightleftharpoons 5$ (circles) and the uncatalysed background (squares). **e**, Kinetics of mixed

(3, circles) and symmetrical (6, crosses; 7, squares) anhydride formation and hydrolysis. Symmetrical anhydrides are consumed through hydrolysis, whereas 3 either hydrolyses or reacts to form 4. Formation and hydrolysis of 3 constitutes an energy-consuming futile cycle. **f**, Free energy profile of ground state species of the anhydride chemical state calculated using (B3LYP/6-31 + G(d,p)/GD3BJ) level of theory with corrections for solvation (PCM in acetonitrile ($\epsilon = 35.688$)). Free energy profile of the diacid chemical state based on experiment. Energies in kJ mol^{-1} . Error bars refer to the measurement of ratios of NMR integrals ($\pm 0.5\%$ relative to starting materials).

nonequilibrium and systems chemistry^{40,48–52}, and we have previously proposed³ that such a fuelling reaction could be suitable for driving coupled reactions out-of-equilibrium.

Mixing 1 and 2 in $\text{CD}_3\text{CN}:\text{D}_2\text{O}$ 3:1 (v/v) at 12.5 mM, led to no detectable (by ^1H nuclear magnetic resonance (NMR) spectroscopy or mass spectrometry) Diels–Alder adduct 5 after 21 days at either 20 °C or 100 °C (Fig. 1c and Supplementary Information Section 2). Experimental determination of the $1 + 2 \rightleftharpoons 5$ equilibrium constant (Supplementary Information Section 2) at various concentrations indicated that the

ratio of $(1 + 2):5$ is $\sim 250:1$ (that is, 0.4% 5) at equilibrium at 12.5 mM, which corresponds to $\Delta G^\circ = +2.8 \text{ kJ mol}^{-1}$.

Addition of diisopropylcarbodiimide (DIC, 1 equiv.) to the non-reacting mixture of 1 and 2 led to the rapid formation of both symmetrical and mixed (3) anhydrides (Fig. 1d,e; DIC was chosen as the fuel due to its modest tendency for *N*-acyl urea formation⁵³). Over the course of several hours, the Diels–Alder adduct 4 was observed to form, presumably from intramolecular cycloaddition of the mixed anhydride, 3, the cycloaddition that did not proceed between the two

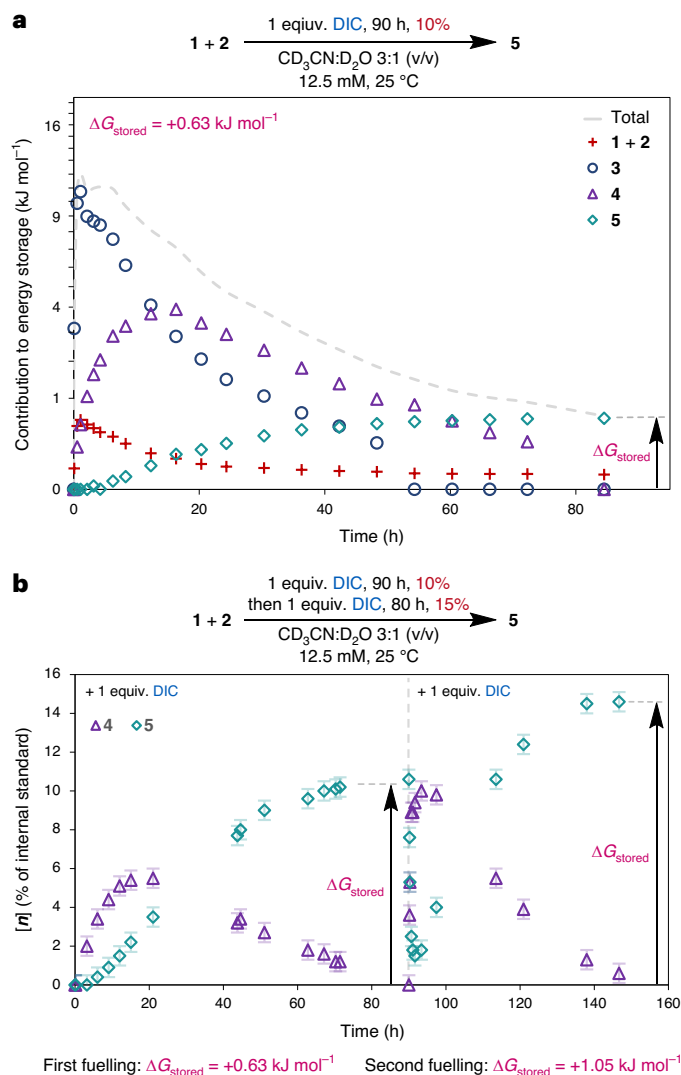


Fig. 3 | Progressive work and energy storage. **a**, The contribution of each species to the energy stored in the out-of-equilibrium reaction network⁵⁴. The vertical axis is non-linear, increasing in increments of y^2 . Reaction conditions: $[1]_0 = [2]_0 = [\text{DIC}]_0 = 12.5 \text{ mM}$, $\text{CD}_3\text{CN:D}_2\text{O 3:1 (v/v)}$, 298 K . **b**, Repeat fuelling of the ratcheted synthesis. Repetition of the fuelling cycle does cumulative chemical work. Reaction conditions: $[1]_0 = [2]_0 = [\text{DIC}]_0 = 12.5 \text{ mM}$, $\text{CD}_3\text{CN:D}_2\text{O 3:1 (v/v)}$, 298 K . Second equivalent of DIC added at $t = 90 \text{ h}$. Error bars refer to the measurement of ratios of NMR integrals ($\pm 0.5\%$ relative to starting materials).

carboxylic acids (**1** and **2**) under the same conditions of solvent, temperature and concentration. Concomitant hydrolysis of the anhydrides led to Diels–Alder adduct **5** in 10% yield (Fig. 2a,c). The structure of **5** was confirmed by two-dimensional NMR and high-resolution mass spectrometry (Supplementary Information Section 3.5). Addition of 2 equiv. (at the start of the reaction) of DIC improved the yield of **5** to 12%. Retro-Diels–Alder of the adduct **5** to reform **1** and **2** occurred spontaneously after the consumption of fuel, with a half-life of 16 days at 20° C , confirming the endergonic nature of the Diels–Alder cycloaddition of **1** and **2** in the absence of chemical fuelling, and the kinetic stability of the Diels–Alder cycloadduct **5** (Fig. 2a–e and Supplementary Information Section 4.1).

Having confirmed that the cycloaddition of **1** and **2** was thermodynamically unfavourable at this concentration (without fuelling), we compared the concentrations of **1**, **2** and **5** at equilibrium with those following chemical fuelling. Calculations⁵⁴ (Fig. 3a and Supplementary Information Section 5) indicated that the Diels–Alder cycloaddition ($\Delta G^\circ = +2.8 \text{ kJ mol}^{-1}$) is ratcheted thermodynamically uphill by

$\Delta G = +0.63 \text{ kJ mol}^{-1}$ (that is, ΔG_{stored}) when 1 equiv. DIC was added. The energy stored over the course of the ratcheted synthesis was quantified using an information thermodynamics approach. As the energy released by the hydration of DIC is -80 kJ mol^{-1} , 0.8% of the energy input is transduced into chemical work in the chemically fuelled cycloaddition to form **5**. The efficiency of energy transduction in the chemically fuelled cycloaddition compares favourably to light and chemically fuelled deracemizations^{24,35}.

Under the reaction conditions, the rate of hydrolysis of the anhydride is rate-limiting for the carbodiimide-to-urea reaction. This results in a fuelling regime in which the system is globally dehydrating for the initial phases of the reaction, followed by globally hydrating once little or no DIC remains. Varying the global conditions of a system over time in order to perform work is characteristic of an energy ratchet mechanism¹¹. Another feature of ratchet mechanisms is that they are repetitive and progressive¹¹, meaning that the fuelling cycle can be repeated to do cumulative work. Indeed, refuelling the endergonic product mixture with a second equivalent of DIC after 90 h (following complete hydrolysis of the anhydride intermediates but before complete thermal relaxation of **5** had occurred; Fig. 3b) increased the yield of **5** to 15% ($\Delta G_{\text{stored}} = +1.05 \text{ kJ mol}^{-1}$; Supplementary Information Section 5.1). This corresponds to two cycles of an energy ratchet mechanism. Following hydrolysis and the relaxation of **1**, **2** and **5** back to equilibrium, repeating the fuelling cycle with a further equivalent of DIC reformed **5** in 7% yield, the reduced conversion due to *N*-acyl urea formation⁵³ (Supplementary Information Section 4.3).

In addition to being thermodynamically uphill, the ratcheted synthesis of the Diels–Alder adduct **5** also proved to be both regio- and stereoselective (Fig. 4a). We could not detect the formation of either *meta* regioisomer of **5** by ^1H NMR, indicating that the ratcheted synthesis is $>99\%$ regioselective for the *ortho*-adduct. Furthermore, we found that **5** is formed under fuelling with 92% stereoselectivity for the *exo*-adduct (Supplementary Information Section 3.6). Molecular modelling suggests that the high selectivity of the ratcheted synthesis for the *exo*- and *ortho*-isomer results from anhydride ring strain disfavoured the *endo* and *meta* Diels–Alder transition states.

To confirm that one of the effects of fuelling is to increase the effective concentration of the diene and dienophile, we heated a neat mixture of **1** and **2** in the absence of solvent at 40° C for 7 days (Fig. 4a and Supplementary Information Section 7). This resulted in a mixture of the four possible isomeric (*endo*-/*exo*-/*ortho*-/*meta*-) Diels–Alder adducts, in 39% total yield (Supplementary Information Section 8). However, ^1H NMR indicated that the thermal solvent-free reaction afforded poor regio- and stereoselectivity, with only 10% of the cycloaddition products formed corresponding to the *exo*- and *ortho*-isomer **5**, a 4% yield from **1** and **2**. The substantial increase in the regio- and stereoselectivity of **5** under chemical fuelling compared with the neat thermal synthesis demonstrates that ratcheting can also be used to distinguish between energetically similar reaction outcomes. This is reminiscent of the way that biology uses kinetic proofreading to distinguish similar monomers in sequence-specific polymer synthesis^{3,4,8}.

As carbodiimides can also drive information ratchet mechanisms^{35,50,51,55}, we explored whether the carbodiimide fuelling cycle in Fig. 1d could promote the formation of **5** at a steady state under fuelling (Fig. 4b). Maintaining a constant concentration of fuel to **1** and **2** by continual addition of DIC to the reaction at a rate of 0.7 equiv. per day led to a steady state of **5** (~4%) in the presence of DIC (Fig. 4d and Supplementary Information Section 9). This is effectively a chemostated^{15,16,56,57} regime, since the concentrations of DIC and D_2O are kept constant and the presence of diisopropyl urea (DIU) does not affect the rate of any of the other processes. As the amount of **5** is below the NMR detection limit at equilibrium (Fig. 1c and Supplementary Information Sections 2 and 4), but is formed under the effectively chemostated conditions, the fuelling cycle must^{15,16,57} possess modest kinetic asymmetry and proceed through an information ratchet^{11,13} mechanism

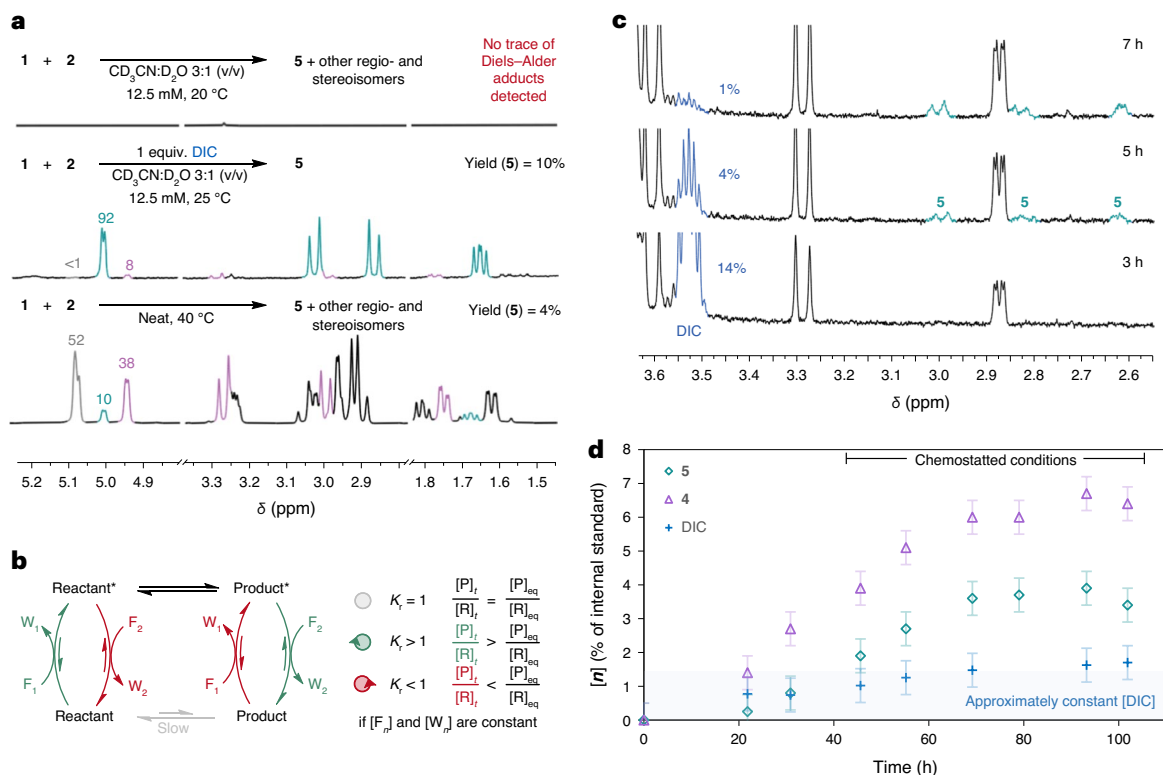


Fig. 4 | Reaction selectivity and mechanistic insights. a, Partial ^1H NMR stackplot (600 MHz, $\text{CD}_3\text{CN:D}_2\text{O}$ 3:1 (v/v), 293 K) showing the regioselectivity, stereoselectivity and yield of the unfueled reaction (top) and the ratcheted synthesis under the same conditions (middle), in comparison with a thermal synthesis (bottom). Numbers denote the relative proportions (%) of the *exo-ortho*- (5, teal), *endo-ortho*- (purple) and *meta*- (grey) isomers. **b**, Ratcheting synthesis through an information ratchet mechanism. An orthogonal fuel ($F_1 \rightarrow W_1$ and $F_2 \rightarrow W_2$) reacting along reaction coordinate 2 can drive an endergonic reaction in reaction coordinate 1, so long as there is kinetic asymmetry ($K_f > 1$) in the fuelling cycle. A thermodynamic preference (a power stroke) in the 'fuelled' (that is, the tethered) state is insufficient to drive the reaction through an information ratchet mechanism (that is, at a chemically fuelled steady state). Kinetic asymmetry is present if the ratio of $[\text{R}]:[\text{P}]$ varies from the

equilibrium distribution under chemostatted conditions (constant fuel and waste concentrations)^{15,16,57}. K_r , ratcheting constant^{15,16,57}; R, reactants; P, product; t , time. **c**, Partial ^1H NMR stackplot (600 MHz, $\text{CD}_3\text{CN:D}_2\text{O}$ 3:1 (v/v), 293 K) after addition of 2 equiv. DIC showing the formation of **5** before the complete consumption of both fuels (DIC and D_2O). Times are approximate; percentages refer to $[\text{DIC}]$ relative to $[\text{DIC}]_0$. Reaction conditions: $[\text{1}] = [\text{2}] = 12.5$ mM, $[\text{DIC}]_0 = 25.0$ mM, $\text{CD}_3\text{CN:D}_2\text{O}$ 3:1 (v/v), 298 K. **d**, The formation of the Diels-Alder adduct **5** under chemostatted conditions. DIC added continually at 0.7 equiv. per day. Reaction conditions: $[\text{1}] = [\text{2}] = 12.5$ mM, $\text{CD}_3\text{CN:D}_2\text{O}$ 3:1 (v/v), 298 K. The concentration of **5** increases over time before reaching a steady state (4%), indicative of an information ratchet mechanism^{15,16,57}. Error bars refer to the measurement of ratios of NMR integrals ($\pm 0.5\%$ relative to starting materials).

(Supplementary Information Section 10). Under non-chemostatted conditions, where the chemical fuel is all added at time zero, the slow hydrolysis step means that the majority of **5** is produced after the consumption of fuel, effectively through an energy ratchet¹¹ mechanism.

Conclusions

The use of ratchet mechanisms to directionally bias stochastic processes is a key principle that underpins the operation of molecular machines^{11–14,35,50,51,55}. The endergonic synthesis of **5** demonstrates how chemically fuelled ratchet mechanisms can also modulate and direct the outcome of organic chemical transformations, just as they do in biology³. The chemically fuelled transformation of **1** and **2** to **5** involves a transiently formed tether between the reactants, which favourably organizes them to bring about the desired transformation. In the energy ratchet mechanism this requires the addition of fuel for each cycle, with the organization of the building blocks causing a power stroke (an energetically downhill reaction) in the tethered intermediate. In the information ratchet pathway, the key to a higher yield is to generate as large a kinetic asymmetry as possible by maximizing the differences in the reaction rates through Curtin-Hammett-type⁵⁷ principles. Despite the modest chemically fuelled yield of **5**, the efficiency of energy transduction from the carbodiimide-to-urea reaction to the Diels-Alder reaction is $\sim 3\text{--}30\times$ greater than the efficiency of a number of previously

reported^{25,26} light-driven deracemization processes (Supplementary Information Section 13). In addition to making the endergonic transformation possible, the steric and chemical constraints necessary for ratcheting also result in improved regio- and stereochemical control in the chemically fuelled Diels-Alder synthesis of **5**.

Like ATP, **5** is thermodynamically unstable under the conditions of its chemically fuelled synthesis. However, the kinetic stability of **5** is higher than that of ATP ($t_{1/2}^{\text{5}} = 16$ days versus $t_{1/2}^{\text{ATP}} \approx 6$ h)²⁰. We note that catalysis of the exergonic retro-Diels-Alder reaction of **5** could allow a suitable molecular machine to harness the chemical energy generated by the ratcheted synthesis to do useful work, rendering **5** a regenerable chemical fuel. However, even though every step of the thermally activated chemically fuelled cycle that makes **5** from **1** and **2** is subject to microreversibility, that does not mean that the products of chemically fuelled endergonic synthesis must necessarily have modest kinetic stability. That simply depends on whether the fastest (fuelled or non-fuelled) reverse pathway has a sufficiently high activation barrier. Such is the case, for example, for the chemically fuelled deracemization of 1-(6'-substituted-phenyl)pyrrole 2,2'-dicarboxylic acid derivatives, where the $t_{1/2}$ of enantiomers of the 6'-ethyl biaryl system is $\sim 22,000$ years (ref. 35). As such, chemically fuelled ratcheted synthesis should prove useful for the endergonic synthesis of products with a range of kinetic stabilities, as well as recyclable fuels²⁰, in

sequence-specific synthesis^{33,34,58,59}, dissipative materials^{40,48,49,52,60,61} and endergonic supramolecular structures^{17–19}. The simplicity of the reactants and fuelling cycle of **5** provides a minimalist demonstration of chemically fuelled ratcheted synthesis that aids its understanding in biology and potential utility in synthesis.

Methods

Stock solutions

Stock solutions of reagents (in CD₃CN) were used when stated: 2-furanacetic acid (**1**, 0.5 M), acrylic acid (**2**, 0.5 M), mesitylene (0.05 M) and DIC (0.5 M). All stock solutions were stored at 5 °C, except acrylic acid, which was freshly distilled immediately before use. Stock solutions were checked for composition and purity before use.

Autonomous fuelling (all of the fuel added at time zero)

Reactions were carried out in a 5 mm NMR tube. Reagents were added from stock solutions, following which CD₃CN and D₂O were added. A 'pre-fuelling' ¹H NMR was recorded; then DIC was added (defined as $t = 0$) from a stock solution, resulting in a 0.5 ml solution. Reactions were monitored periodically by ¹H NMR. The experiments carried out at 20 °C were kept in the temperature-controlled laboratory and analysed at 20 °C. The reactions carried out at 25 °C were kept within the temperature-controlled NMR probe for the duration of the experiment.

Pseudo-chemostated fuelling

In a 250-ml flask under a N₂ atmosphere, freshly distilled acrylic acid (**2**) (216 mg, 2.50 mmol, 1 equiv.), 2-furanacetic acid (**1**) (315 mg, 2.50 mmol, 1 equiv.) and mesitylene (30 mg, 0.25 mmol, 10 mol%) were dissolved in CD₃CN:D₂O 3:1 (v/v) (12.5 mM, 200 ml). The solution was stirred at 20 °C, and DIC (0.5 M in CD₃CN) (0.7 equiv. per day) was added continuously over a period of 6 days using a syringe pump. Care was taken to ensure no large drops formed by positioning the needle against the wall of the flask. Samples (0.5 ml) were taken periodically and analysed by ¹H NMR.

Data availability

The data that support the findings of this study are available within the paper and its Supplementary Information. Source data are provided with this paper.

References

1. Russell, J. B. & Cook, G. M. Energetics of bacterial growth: balance of anabolic and catabolic reactions. *Microbiol. Rev.* **59**, 48–62 (1995).
2. Wang, P.-Z., Xiao, W.-J. & Chen, J.-R. Light-empowered contra-thermodynamic stereochemical editing. *Nat. Rev. Chem.* **7**, 35–50 (2023).
3. Borsley, S., Gallagher, J. M., Leigh, D. A. & Roberts, B. M. W. Ratcheting synthesis. *Nat. Rev. Chem.* **8**, 8–29 (2024).
4. Sangchai, T., Al Shehimi, S., Penocchio, E. & Ragazzon, G. Artificial molecular ratchets: tools enabling endergonic processes. *Angew. Chem. Int. Ed.* **62**, e202309501 (2023).
5. Walsh, C. T., Tu, B. P. & Tang, Y. Eight kinetically stable but thermodynamically activated molecules that power cell metabolism. *Chem. Rev.* **118**, 1460–1494 (2018).
6. Cartling, B. & Ehrenberg, A. A molecular mechanism of the energetic coupling of a sequence of electron transfer reactions to endergonic reactions. *Biophys. J.* **23**, 451–461 (1978).
7. Mitchell, P. Coupling of phosphorylation to electron and hydrogen transfer by a chemi-osmotic type of mechanism. *Nature* **191**, 144–148 (1961).
8. Hopfield, J. J. Kinetic proofreading: a new mechanism for reducing errors in biosynthetic processes requiring high specificity. *Proc. Natl Acad. Sci. USA* **71**, 4135–4139 (1974).
9. Holden, H. M., Rayment, I. & Thoden, J. B. Structure and function of enzymes of the Leloir pathway for galactose metabolism. *J. Biol. Chem.* **278**, 43885–43888 (2003).
10. Amano, S., Borsley, S., Leigh, D. A. & Sun, Z. Chemical engines: driving systems away from equilibrium through catalyst reaction cycles. *Nat. Nanotechnol.* **16**, 1057–1067 (2021).
11. Kay, E. R., Leigh, D. A. & Zerbetto, F. Synthetic molecular motors and mechanical machines. *Angew. Chem. Int. Ed.* **46**, 72–191 (2007).
12. Erbas-Cakmak, S., Leigh, D. A., McTernan, C. T. & Nussbaumer, A. L. Artificial molecular machines. *Chem. Rev.* **115**, 10081–10206 (2015).
13. Astumian, R. D. Kinetic asymmetry allows macromolecular catalysts to drive an information ratchet. *Nat. Commun.* **10**, 3837 (2019).
14. Astumian, R. D., Mukherjee, S. & Warshel, A. The physics and physical chemistry of molecular machines. *ChemPhysChem* **17**, 1719–1741 (2016).
15. Ragazzon, G. & Prins, L. J. Energy consumption in chemical fuel-driven self-assembly. *Nat. Nanotechnol.* **13**, 882–889 (2018).
16. Das, K., Gabrielli, L. & Prins, L. J. Chemically fueled self-assembly in biology and chemistry. *Angew. Chem. Int. Ed.* **60**, 20120–20143 (2021).
17. Chen, X., Würbser, M. A. & Boekhoven, J. Chemically fueled supramolecular materials. *Acc. Mater. Res.* **4**, 416–426 (2023).
18. Sorrenti, A., Leira-Iglesias, J., Markvoort, A. J., de Greef, T. F. A. & Hermans, T. M. Non-equilibrium supramolecular polymerization. *Chem. Soc. Rev.* **46**, 5476–5490 (2017).
19. Sharko, A., Livitz, D., De Piccoli, S., Bishop, K. J. M. & Hermans, T. M. Insights into chemically fueled supramolecular polymers. *Chem. Rev.* **122**, 11759–11777 (2022).
20. Borsley, S., Leigh, D. A. & Roberts, B. M. W. Chemical fuels for molecular machinery. *Nat. Chem.* **14**, 728–738 (2022).
21. Parrondo, J. M. R. & Dinis, L. Brownian motion and gambling: from ratchets to paradoxical games. *Contemp. Phys.* **45**, 147–157 (2004).
22. Kurtz, T. G. The relationship between stochastic and deterministic models for chemical reactions. *J. Chem. Phys.* **57**, 2976–2978 (1972).
23. Carrillo, L., Escobar, J. A., Clempner, J. B. & Poznyak, A. S. Optimization problems in chemical reactions using continuous-time Markov chains. *J. Math. Chem.* **54**, 1233–1254 (2016).
24. Wang, H., Tian, Y.-M. & König, B. Energy- and atom-efficient chemical synthesis with endergonic photocatalysis. *Nat. Rev. Chem.* **6**, 745–755 (2022).
25. Hölzl-Hobmeier, A. et al. Catalytic deracemization of chiral allenes by sensitized excitation with visible light. *Nature* **564**, 240–243 (2018).
26. Shin, N. Y., Ryss, J. M., Zhang, X., Miller, S. J. & Knowles, R. R. Light-driven deracemization enabled by excited-state electron transfer. *Science* **366**, 364–369 (2019).
27. Huang, M., Zhang, L., Pan, T. & Luo, S. Deracemization through photochemical E/Z isomerization of enamines. *Science* **375**, 869–874 (2022).
28. Molloy, J. J. et al. Boron-enabled geometric isomerization of alkenes via selective energy-transfer catalysis. *Science* **369**, 302–306 (2020).
29. Zhao, K. & Knowles, R. R. Contra-thermodynamic positional isomerization of olefins. *J. Am. Chem. Soc.* **144**, 137–144 (2021).
30. Singh, K., Staig, S. J. & Weaver, J. D. Facile synthesis of Z-alkenes via uphill catalysis. *J. Am. Chem. Soc.* **136**, 5275–5278 (2014).
31. Zhu, X.-G., Long, S. P. & Ort, D. R. What is the maximum efficiency with which photosynthesis can convert solar energy into biomass? *Curr. Opin. Biotechnol.* **19**, 153–159 (2008).
32. Biagini, C. & Di Stefano, S. Abiotic chemical fuels for the operation of molecular machines. *Angew. Chem. Int. Ed.* **59**, 8344–8354 (2020).

33. Bar-Nahum, G. et al. A ratchet mechanism of transcription elongation and its control. *Cell* **120**, 183–193 (2005).
34. Spirin, A. S. & Finkelstein, A. V. in *Biology: Workshop of the Cell* (ed. Frank J.) 158–190 (Cambridge Univ. Press, 2012).
35. Borsley, S., Kreidt, E., Leigh, D. A. & Roberts, B. M. W. Autonomous fuelled directional rotation about a covalent single bond. *Nature* **604**, 80–85 (2022).
36. Lackner, A. D., Samant, A. V. & Toste, F. D. Single-operation deracemization of 3*H*-indolines and tetrahydroquinolines enabled by phase separation. *J. Am. Chem. Soc.* **135**, 14090–14093 (2013).
37. Ji, Y., Shi, L., Chen, M.-W., Feng, G.-S. & Zhou, Y.-G. Concise redox deracemization of secondary and tertiary amines with a tetrahydroisoquinoline core via a nonenzymatic process. *J. Am. Chem. Soc.* **137**, 10496–10499 (2015).
38. Marchetti, T., Frezzato, D., Gabrielli, L. & Prins, L. J. ATP drives the formation of a catalytic hydrazone through an energy ratchet mechanism. *Angew. Chem. Int. Ed.* **62**, e202307530 (2023).
39. Corey, E. J. Catalytic enantioselective Diels–Alder reactions: methods, mechanistic fundamentals, pathways, and applications. *Angew. Chem. Int. Ed.* **41**, 1650–1667 (2002).
40. Würbser, M. A. et al. Chemically fueled block copolymer self-assembly into transient nanoreactors. *ChemSystChem* **3**, e2100015 (2021).
41. Cox, L. R. & Ley, S. V. in *Templated Organic Synthesis* Ch. 10 (eds Diederich, F. & Stang, P. J.) 275–306 (Wiley-VCH, 2000).
42. Ahrendt, K. A., Borths, C. J. & MacMillan, D. W. C. New strategies for organic catalysis: the first highly enantioselective organocatalytic Diels–Alder reaction. *J. Am. Chem. Soc.* **122**, 4243–4244 (2000).
43. Boul, P. J., Reutenauer, P. & Lehn, J. M. Reversible Diels–Alder reactions for the generation of dynamic combinatorial libraries. *Org. Lett.* **7**, 15–18 (2005).
44. Narasaka, K., Shimada, S., Osoda, K. & Iwasawa, N. Phenylboronic acid as a template in the Diels–Alder reaction. *Synthesis* **1991**, 1171–1172 (1991).
45. Nicolau, K. C. et al. Total synthesis of taxol. 2. Construction of A and C ring intermediates and initial attempts to construct the ABC ring system. *J. Am. Chem. Soc.* **117**, 634–644 (1995).
46. Zubkov, F. I., Nikitina, E. V. & Varlamov, A. V. Thermal and catalytic intramolecular [4+2]-cycloaddition in 2-alkenylfurans. *Russ. Chem. Rev.* **74**, 639–669 (2005).
47. Tromp, R. A., Brussee, J. & van der Gen, A. Stereochemistry of intramolecular Diels–Alder furan (IMDAF) reactions of furyl-substituted chiral ethanolamides. *Org. Biomol. Chem.* **1**, 3592–3599 (2003).
48. Tena-Solsona, M. et al. Non-equilibrium dissipative supramolecular materials with a tunable lifetime. *Nat. Commun.* **8**, 15895 (2017).
49. Kariyawasam, L. S. & Hartley, C. S. Dissipative assembly of aqueous carboxylic acid anhydrides fueled by carbodiimides. *J. Am. Chem. Soc.* **139**, 11949–11955 (2017).
50. Borsley, S., Leigh, D. A. & Roberts, B. M. W. A doubly kinetically-gated information ratchet autonomously driven by carbodiimide hydration. *J. Am. Chem. Soc.* **143**, 4414–4420 (2021).
51. Binks, L. et al. The role of kinetic asymmetry and power strokes in an information ratchet. *Chem* **9**, 2902–2917 (2023).
52. Hossain, M. M., Jayalath, I. M., Baral, R. & Hartley, C. S. Carbodiimide-induced formation of transient polyether cages. *ChemSystChem* **4**, e202200016 (2022).
53. Chen, X., Soria-Carrera, H., Zozulia, O. & Boekhoven, J. Suppressing catalyst poisoning in the carbodiimide-fueled reaction cycle. *Chem. Sci.* **14**, 12653–12660 (2023).
54. Penocchio, E., Rao, R. & Esposito, M. Thermodynamic efficiency in dissipative chemistry. *Nat. Commun.* **10**, 3865 (2019).
55. Liu, E. et al. A molecular information ratchet using a cone-shaped macrocycle. *Chem* **9**, 1147–1163 (2023).
56. Aprahamian, I. & Goldup, S. M. Non-equilibrium steady states in catalysis, molecular motors, and supramolecular materials: why networks and language matter. *J. Am. Chem. Soc.* **145**, 14169–14183 (2023).
57. Amano, S. et al. Using catalysis to drive chemistry away from equilibrium: relating kinetic asymmetry, power strokes, and the Curtin–Hammett principle in Brownian ratchets. *J. Am. Chem. Soc.* **144**, 20153–20164 (2022).
58. Lewandowski, B. et al. Sequence-specific peptide synthesis by an artificial small-molecule machine. *Science* **339**, 189–193 (2013).
59. Kassem, S. et al. Stereodivergent synthesis with a programmable molecular machine. *Nature* **549**, 374–378 (2017).
60. Singh, N., Lopez-Acosta, A., Formon, G. J. & Hermans, T. M. Chemically fueled self-sorted hydrogels. *J. Am. Chem. Soc.* **144**, 410–415 (2021).
61. Boekhoven, J., Hendriksen, W. E., Koper, G. J., Eelkema, R. & van Esch, J. H. Transient assembly of active materials fueled by a chemical reaction. *Science* **349**, 1075–1079 (2015).
62. Tordini, F. et al. Theoretical study of hydration of cyanamide and carbodiimide. *J. Phys. Chem. A* **107**, 1188–1196 (2003).

Acknowledgements

We thank the Engineering and Physical Sciences Research Council (EPSRC; grant numbers EP/PO27067/1 and EP/S023755/1), and the European Research Council (ERC; Advanced Grant number 786630) for funding, the University of Manchester's Department of Chemistry Services for mass spectrometry, B. M. W. Roberts and E. Penocchio for discussions on nonequilibrium thermodynamics, and S. Borsley and M. J. Power for other useful discussions. D.A.L. is a Royal Society Research Professor.

Author contributions

J.M.G. conceived the project. E.O., J.M.G., A.B. and T.W.M. designed and carried out the experiments. D.A.L. directed the research. All authors contributed to the analysis of the results and the writing of the manuscript.

Competing interests

The authors declare no competing interests.

Additional information

Supplementary information The online version contains supplementary material available at <https://doi.org/10.1038/s44160-024-00493-w>.

Correspondence and requests for materials should be addressed to David A. Leigh.

Peer review information *Nature Synthesis* thanks Job Boekhoven, Stefano Di Stefano and the other, anonymous, reviewer(s) for their contribution to the peer review of this work. Primary Handling Editor: Alison Stoddart, in collaboration with the *Nature Synthesis* team.

Reprints and permissions information is available at www.nature.com/reprints.

Publisher's note Springer Nature remains neutral with regard to jurisdictional claims in published maps and institutional affiliations.

Open Access This article is licensed under a Creative Commons Attribution 4.0 International License, which permits use, sharing, adaptation, distribution and reproduction in any medium or format, as long as you give appropriate credit to the original author(s) and the source, provide a link to the Creative Commons licence, and indicate

if changes were made. The images or other third party material in this article are included in the article's Creative Commons licence, unless indicated otherwise in a credit line to the material. If material is not included in the article's Creative Commons licence and your intended use is not permitted by statutory regulation or exceeds the permitted

use, you will need to obtain permission directly from the copyright holder. To view a copy of this licence, visit <http://creativecommons.org/licenses/by/4.0/>.

© The Author(s) 2024